Received: 21 January 2021 | Revised: 12 April 2021 | Accepted: 20 May 2021

DOI: 10.1111/clr.13792

ORIGINAL ARTICLE

CLINICAL ORAL IMPLANTS RESEARCH WILEY

Bone healing around titanium implants in a preclinical model of bile duct ligation-induced liver injury

Reza Talebian[1,2] | Carina Kampleitner[3,4,5] | Benedikt Sagl[6] | Ulrike Kuchler[7] | Ahmad Reza Dehpour[2,8] | Reinhard Gruber[1,5,9]

[1]Department of Oral Biology, University Clinic of Dentistry, Medical University of Vienna, Vienna, Austria

[2]Experimental Medicine Research Center, School of Medicine, Tehran University of Medical Sciences, Tehran, Iran

[3]Karl Donath Laboratory for Hard Tissue and Biomaterial Research, University Clinic of Dentistry, Medical University of Vienna, Vienna, Austria

[4]Ludwig Boltzmann Institute for Experimental and Clinical Traumatology, AUVA Research Center, Vienna, Austria

[5]Austrian Cluster for Tissue Regeneration, Vienna, Austria

[6]Department of Prosthodontics, University Clinic of Dentistry, Medical University of Vienna, Vienna, Austria

[7]Department of Oral Surgery, University Clinic of Dentistry, Medical University of Vienna, Vienna, Austria

[8]Department of Pharmacology, School of Medicine, Tehran University of Medical Sciences, Tehran, Iran

[9]Department of Periodontology, School of Dental Medicine, University of Bern, Bern, Switzerland

Correspondence
Reinhard Gruber, Department of Oral Biology, University Clinic of Dentistry, Medical University of Vienna, Sensengasse 2a, 1090 Vienna, Austria.
Email: reinhard.gruber@meduniwien.ac.at

Ahmad Reza Dehpour, Department of Pharmacology, School of Medicine, Tehran University of Medical Sciences, P.O. Box: 13145–784, Tehran, Iran.
Email: dehpour@yahoo.com

Abstract

Objectives: Chronic liver disease increases the risk for periodontal disease and osteoporotic fractures, but its impacts on bone regeneration remain unknown. Herein, we studied the impact of liver cirrhosis on peri-implant bone formation.

Material and Methods: A total of 20 male Wistar rats were randomly divided into two groups: one with the common bile duct ligated (BDL) and the respective sham-treated control group (SHAM). After four weeks of disease induction, titanium mini-screws were inserted into the tibia. Successful induction of liver cirrhosis was confirmed by the presence of clinical symptoms. Another four weeks later, peri-implant bone volume per tissue volume (BV/TV) and bone-to-implant contact (BIC) were determined by histomorphometric analysis.

Results: Peri-implant bone formation was not significantly different between the SHAM and BDL groups. In the cortical compartment, the median percentage of peri-implant new bone was 10.1% (95% CI of mean 4.0–35.7) and 22.5% (13.8–30.6) in the SHAM and BDL groups, respectively ($p = .26$). Consistently, the new bone in direct contact with the implant was 18.1% (0.4–37.8) and 23.3% (9.2–32.8) in SHAM and BDL groups, respectively ($p = .38$). When measuring the medullary compartment, the new bone area was 7.1% (4.8–10.4) and 10.4% (7.2–13.5) in the SHAM and BDL groups, respectively ($p = .17$). Medullary new bone in direct contact with the implant was 10.0% (1.2–50.4) and 20.6% (16.8–35.3) in SHAM and BDL groups, respectively, and thus comparable between the two groups ($p = .46$).

Conclusions: Bile duct ligation has no significant impact on the early stages of peri-implant bone formation.

KEYWORDS

bile duct ligation, bone regeneration, implant, liver cirrhosis, osseointegration, rat, tibia

1 | INTRODUCTION

Chronic liver disease, and in particular liver cirrhosis, has become a public health concern and a known source of morbidity and mortality (Schuppan & Afdhal, 2008). Apart from alcohol consumption, hepatitis B, C, and fatty liver disease can cause liver cirrhosis. The prevalence of cirrhosis in industrialized countries is estimated at 0.3% (Scaglione et al., 2015). Regardless of the etiology, cirrhosis doubles the risk of pathological fractures (Handzlik-Orlik et al., 2016; Hidalgo et al., 2020; Luxon, 2011). Moreover, cirrhotic patients with fractures had significantly higher mortality and hospitalization rate than the regular population (Mavilia et al., 2019).

Cirrhosis was also identified being a risk factor for periodontal disease (Chen et al., 2020) and tooth loss (Yoon et al., 2016). Considering that osseointegration of dental implants requires bone regeneration by intramembranous ossification (Vasak et al., 2014), the question of if liver cirrhosis affects peri-implant bone formation seems relevant. Liver cirrhosis and immunosuppression in liver transplant patients were not identified as being a risk factor for implant failure (Gu & Yu, 2011; Paredes et al., 2017; Schimmel et al., 2018). Hepatic osteodystrophy induced by a choline-deficient diet, however, caused impaired peri-implant bone healing (Gorustovich et al., 2003). Whether cirrhosis affects the peri-implant bone formation of dental implants remains unclear.

Cirrhosis can be induced by bile duct ligation (BDL) in preclinical models that develops clinical symptoms such as ascites, weight and muscle loss, and jaundice caused by high bilirubin levels. This model was originally described in 1984 (Kountouras et al., 1984) and was established by Dehpour et al. to study the impact of the opioidergic systems on bone loss (Doustimotlagh et al., 2017; Moradi et al., 2019), angiogenesis (Faramarzi et al., 2009), and morphological changes in the retina (Algazo et al., 2015). There is, however, some inconsistency with respect to bone biology as in BDL rats; some bone turnover markers were increased (Doustimotlagh et al., 2017, 2018) but the bone-specific marker, osteocalcin, remained unchanged (Veidal et al., 2010). Furthermore, BDL supported orthodontic tooth movement (Shirazi et al., 2008), but neither the cortical and trabecular thickness (Doustimotlagh et al., 2017) nor the femoral breaking strength was significantly affected one month following BDL (Moradi et al., 2019). MicroCT also revealed that six weeks post BDL, only minor changes in the trabecular structure become visible and the relative bone volume remains unchanged (Xu et al., 2020). Thus, a possible impact of BDL-induced cirrhosis on peri-implant bone formation cannot be predicted.

The rat tibia implantation model not necessarily reflects the unique situation of the alveolar bone but is a useful well-established model to study basic peri-implant bone regeneration, particularly allowing to distinguish cortical and medullary bone formation. This model has already been applied by our group to evaluate the effects of aging (Mair et al., 2009), diabetes mellitus on anabolic activity of PTH (Kuchler et al., 2011; Rybaczek et al., 2015), and to study the impact of vitamin D deficiency on peri-implant bone formation (Dvorak et al., 2012). Thus, the overall aim of this study was to evaluate the possible effects of BDL-induced cirrhosis on the early stages of peri-implant bone formation in the rat tibia.

2 | MATERIAL AND METHODS

2.1 | Induction of liver cirrhosis through ligation of bile duct

The present study was conducted at the Experimental Medicine Research Center of the School of Medicine, Tehran University of Medical Sciences, following the ARRIVE guidelines. Approval of the study protocol was obtained by the local ethical committee at the Tehran University of Medical Sciences (IR.TUMS.MEDICINE.REC.1397.655). The animals were treated according to the guidelines for animal care with free access to water and a standard diet. In brief, 20 male Wistar rats (230–250 g) obtained from the Pasteur Institute of Iran were randomly allocated into two groups: (I) Bile duct ligated group (BDL) in which cirrhosis was induced by ligation of the bile duct in ten Wistar rats. (II) Sham-operated group (SHAM) in which manipulation of the bile duct without any ligation and resection was performed. A standard and highly established preclinical model of cholestasis was applied for induction of liver cirrhosis (Derakhshanian et al., 2013; Hosseini-Chegeni et al., 2019; Rahimi et al., 2018). Briefly, general anesthesia was achieved by intraperitoneal injection of 100 mg/kg ketamine hydrochloride (Pharmacia & Upjohn) and 5 mg/kg xylazine (Bayer). Laparotomy was done for all of the 20 rats of the two groups. The manipulation of the common bile duct was performed for the SHAM group. Neither ligation nor resection of the bile duct was involved. In the BDL group, the common bile duct was doubly ligated with 3–0 silk thread and then sectioned between the ligatures. The incision was closed with absorbable 5–0 silk thread in two layers. Successful induction of liver cirrhosis was confirmed based on the clinical symptoms. Four weeks after the surgery, BDL rats showed pronounced weight loss, muscle wasting, jaundice, ascites, and hepatocellular disintegration.

2.2 | Implant insertion

Insertion of the implants was done four weeks following the SHAM and BDL surgeries after successful induction of the liver cirrhosis. Preoperatively, all animals received an intraperitoneal injection of 100 mg/kg ketamine hydrochloride (Pharmacia & Upjohn) and 5 mg/kg xylazine (Bayer). An incision was made over the proximal metaphysis of the left tibia, and the muscles and periosteum were displaced. A hole was drilled 10 mm below the knee joint, and a titanium mini screw (Ti6Al4V; hardness 30; diameter 1 mm, length 3 mm; Medos Medizintechnik) with a machined surface was inserted. Wounds were closed with absorbable sutures (Vicryl 4–0; Ethicon GmbH). After four weeks, the animals were sacrificed via inhalation of CO_2

gas followed by decapitation. The specimens were fixed in 10% neutral-buffered formalin (Sigma-Aldrich).

2.3 | Hard tissue sample processing

Following the fixation in neutral-buffered formalin, the tibiae were dehydrated in ascending grades of alcohol and embedded in light-curing resin (Technovit 7200 VLC + BPO; Kulzer & Co.). Blocks were further processed using Exakt cutting and grinding equipment (Exakt Apparatebau). Thin-ground sections were prepared along the implant axis and the longitudinal axis of the tibia and stained with Levai–Laczko dye. The slices were scanned using an Olympus BX61VS digital virtual microscopy system (DotSlide 2.4, Olympus) with a 20× objective resulting in a resolution of 0.32 μm per pixel and then interactively classified using Adobe Photoshop® software (Adobe). Histomorphometric analysis was blinded and performed at three regions of interest (ROIs), representing the medullary, cortical, and periosteal compartments.

2.4 | Histomorphometric analysis

The implant surface in contact with mineralized old and new bones referred to as the "bone-to-implant contact" (BIC), was calculated as a percentage. "Bone volume per tissue volume" (BV/TV) was determined within a distance of 200 μm immediately adjacent to the implant surface and indicated as a percentage (Figure 1). BV/TV was calculated by dividing the area of bone volume (BV) by the total tissue volume (TV) present in the region of interest. BIC and BV/TV were determined in the medullary, cortical, and periosteal compartments. The medullary region of interest was limited to 1 mm adjacent to the cortical region. The periosteal region of interest was limited to the 200 μm outside the cortical region. Measurements were performed using Definiens Developer XD 2.7 (Definiens AG). Colors in the manually drawn segmentation were thresholded. Measurement was then limited to the area within 200 μm of the implant. From the borders of the cortical region, the periosteal region was created by measuring 200 μm away from the outer border of the cortex. In the same way, the medullary region was created by measuring 1,000 μm from the inner border of the cortex. Areas were measured by counting the pixels of each class contained in the three different regions. Contact length between the implant and the different tissues was calculated by measuring a polygonal surface, which was fitted to approximate the real implant surface.

2.5 | Statistics

Based on the study by Kuchler et al. in which BV/TV was calculated as the primary endpoint for 20% with 4% of standard deviation (*SD*), we assumed 15% of BV/TV for cirrhosis. To reach the power of 80%, considering a 95% of confidence interval (alpha = 0.05), the total number of 20 animals was divided equally into two groups named SHAM and BDL. Mann–Whitney U test was applied to compare seven animals per group as we excluded three implants per group at the level of histological evaluation because of the bicortical and metaphyseal position that might have affected the histomorphometric outcome. The p-values of all tests are indicated in the figures.

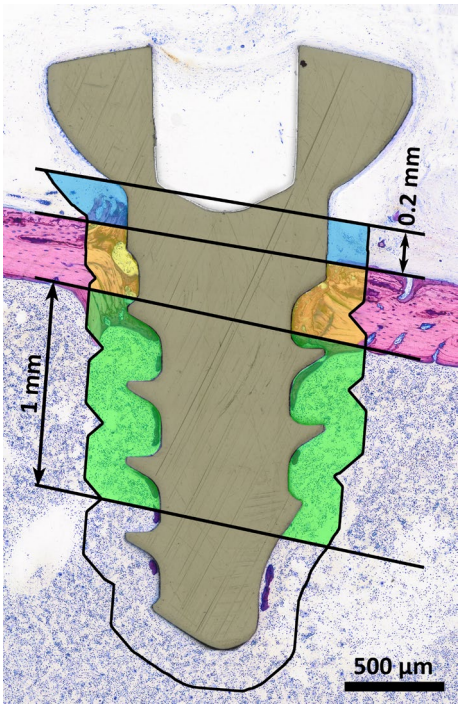

FIGURE 1 Regions of interest in the histomorphometric analysis. The tissue surrounding the implant was segmented into following three regions of interest: the periosteal (blue), the cortical (yellow), and the medullary region (green), the latter extending 1 mm into the bone marrow. In all three regions, we distinguished between new and old bone based on the histological staining intensity and calculated the "bone volume per tissue volume" (BV/TV) within the region 200 μm immediately adjacent to the implant surface. We also determined the "bone-to-implant contact" (BIC) representing the relative coverage of the implant surface with bone

3 | RESULTS

3.1 | Bile duct ligation, induction of cirrhosis, and side effects

Four weeks after BDL surgery, evaluation of the rats for jaundice, ascites, weight, and muscle loss was done to confirm the successful induction of cirrhosis. The BDL but not the SHAM-operated group had symptoms of hepatic failure such as the formation of ascites accumulate liquid in the abdominal cavity in contrast to a normal rat (Figure 2a). In our previous studies, we have confirmed that BDL greatly decreased body weight and increase plasma bilirubin and liver enzymes such as alanine-, aspartate-, and alkaline

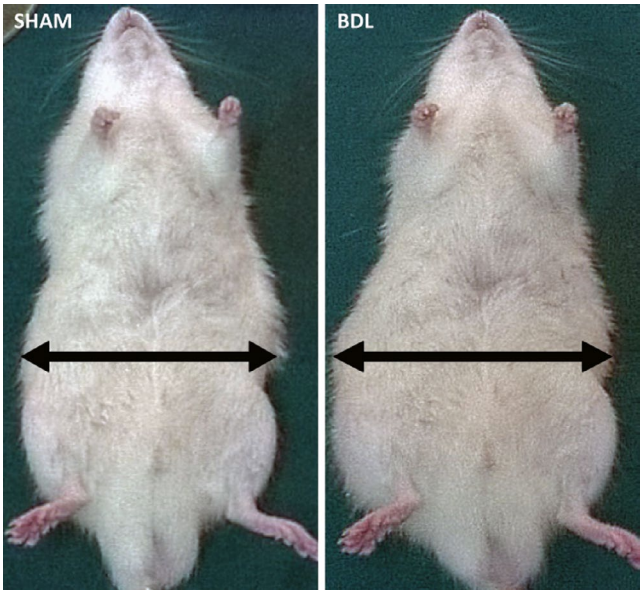

FIGURE 2 Bile duct ligation caused the swollen abdominal cavity as sign of cirrhosis. Cirrhosis was induced by bile duct ligation (BDL) in Wistar rats. Manipulation but not ligation or dissection of common bile duct was performed for the SHAM group. The confirmation of the successful induction of liver cirrhosis was based on the clinical symptoms. Four weeks after the surgery, the SHAM group appeared normal while the BDL rats experienced the formation of ascites, the accumulating liquid in the abdominal cavity

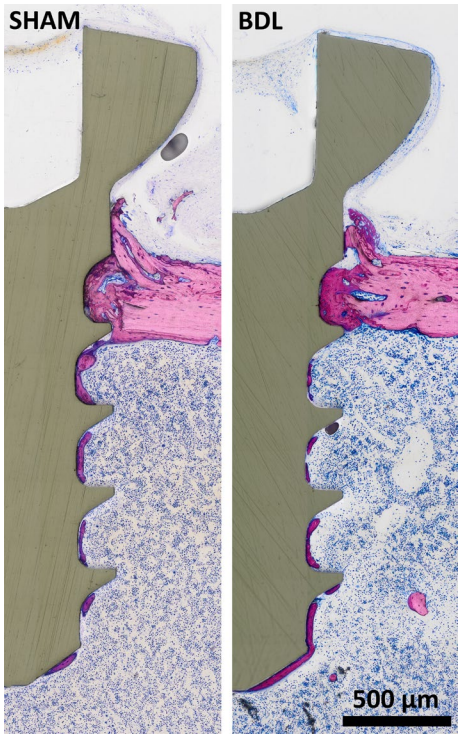

FIGURE 3 Overview of histological analysis of the implants after healing. Histological picture of the implant in the tibia, highlighting the region of interest. SHAM operation surgery and bile duct ligation were performed four weeks prior to implant placement. After another four weeks of healing, thin-ground sections were prepared along the implant axis and the longitudinal axis of the tibia and stained with Levai-Laczko dye. The cortical bone providing the mechanical support of the implant is clearly visible. Also, the bone formed on the surface of the implant in the medullary compartment is distinguishable based on the darker purple staining. In contrast, the pre-existing cortical bone is stained faintly purple. The remaining bone marrow appears blue and cell-rich. There are no obvious differences with respect to peri-implant bone formation when SHAM and BDL groups are compared

aminotransferase and g-glutamyl transferase (Doustimotlagh et al., 2017; Moradi et al., 2019). Histology of the liver revealed cytoplasmic degeneration and pyknotic nuclei in the BDL but not in the SHAM group (Ghiassy et al., 2017). Under these conditions, the insertion of the implants into the tibia was performed. No animals died during the surgery and the follow-up period. The healing was uneventful, with no wound dehiscence in the SHAM and the BDL groups.

3.2 | Histological analysis of the implants after healing

Next, we evaluated the impact of cirrhosis induced by BDL on peri-implant bone formation at the histological level. The overview showing the titanium miniscrews with a turned surface being firmly placed in the cortex of the tibia with most of the threads inserted in the medullary compartment. A similar picture was obtained when analyzing the SHAM group of implants. The overview already exposes the formation of new bone that is indicated by the dark purple stain in the cortical and medullary compartments (Figure 3). Figure 4 is a higher magnification view highlighting the faintly and darker purple staining of the pre-existing and the new bone, respectively, that could thus be distinguished in the quantitative analysis. The histology shows viable osteocytes and bone formation indicated by osteoblast seams, as well as direct contact of the new bone with the implant in the SHAM and the BDL group (Figure 4).

3.3 | Histomorphometric analysis of the implants after healing—the medullary bone

A morphometric analysis of the medullary compartment that indicates almost exclusively new bone formation was performed. When measuring the newly formed bone in the medullary compartment, the BV/TV was 7.1% (4.8–10.4) and 10.4% (7.2–13.5) in the SHAM and BDL groups, respectively ($p = .165$). In line with the amount of bone, also the new bone in direct contact with the implant, the BIC, was 10.0% (1.2–50.4) and 20.6% (16.8–35.3) in the SHAM and BDL groups, respectively, and thus comparable between the two groups ($p = .456$). Considering that the medulla of the diaphysis is devoid of

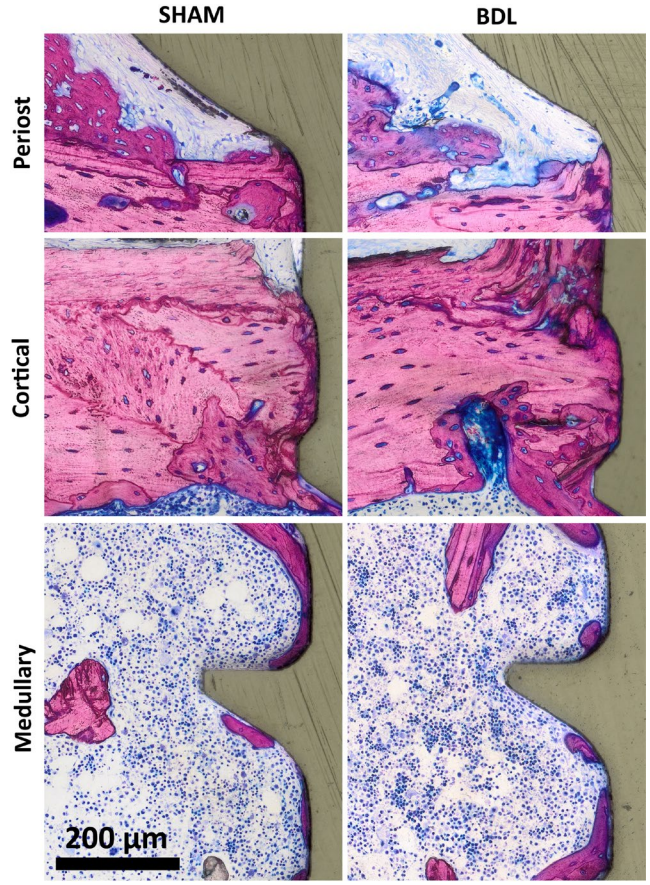

FIGURE 4 Detailed histological analysis of the implants after healing. High magnification images of the thin-ground sections stained with Levai–Laczko dye provide insights into the three regions of interest, the periosteal, cortical, and medullary compartments. Four weeks after SHAM and BDL operation surgeries, implants were placed, and after another four weeks of healing, histological analysis was performed. (I) In the periosteal region, old pre-existing bone and new bone that can be distinguished by its strong purple hue from the faintly stained old bone can be observed. Also, noticeable are the characteristic large osteocytes lacunae of immature woven bone that is laid down on the surface of the old bone. (II) The cortical compartment revealed mainly old cortical bone but also areas of new bone formation. Signs of remodeling that has replaced the old with new bone are visible in the SHAM and BDL groups. (III) The medullary compartment shows the cell-rich matrix characteristic for the marrow space that surrounds the new bone laid down onto the surface of the titanium screws. Also fragments of old bone which were formed during implant placement surgery are visible. Again, no obvious differences are visible when comparing the images of the SHAM with those of the BDL group

pre-existing bone, the occurrence of pristine cortical bone was negligible, with BV/TV reaching 1.8% (0.3–4.7) and 2.7% (1.0–4.5) in the SHAM and BDL groups, respectively (Figure 5). Thus, in the medullary compartment, there was no obvious effect of cirrhosis induced by BDL on the early stages of peri-implant bone formation in the rat tibia implantation model.

3.4 | Histomorphometric analysis of the implants after healing—the cortical bone

When focusing on the amount of newly formed bone in the cortical compartment, the median percentage of bone, indicated as BV/TV was 10.1% (95% CI of mean 4.0–35.7) and 22.5% (13.8–30.6) in the SHAM and BDL groups, respectively ($p = .259$). Consistently, the new bone in direct contact with the implant, the BIC, was 18.1 (0.4–37.8) and 23.3 (9.2–32.8) in the SHAM and BDL groups, respectively, and thus comparable between the two groups ($p = .383$). As expected, the overall amount (BV/TV) and thus the BIC of old pristine cortical bone were obviously higher than those of the new bone, but again, not significantly affected by cirrhosis induced by BDL (Figure 6).

3.5 | Histomorphometric analysis of the implants after healing—the periosteal bone

Finally, we evaluated bone formation within the periosteal region of interest. Figure 7 shows that the newly formed bone in the periosteal compartment, the BV/TV, was 20.1% (6.7–41.6) and 3.9% (−3.9–32.2) in the SHAM and BDL groups, respectively ($p = .20$). The new bone in direct contact with the implant, the BIC, was 0 (−2.9–30.2) and 0 (−1.5–6.2) in SHAM and BDL groups, and thus comparable between the two groups ($p = .57$). As summarized in Figure 7, there was a high variation within each group and no clear trend on an association with cirrhosis induced by BDL in the periosteal compartment.

4 | DISCUSSION

There are many reasons why metabolic changes that are caused by liver cirrhosis could have an impact on the early stages of osseointegration. Cirrhosis is a risk factor for osteoporotic fractures suggesting an effect of cirrhosis on bone metabolism that may extend toward bone regeneration (Handzlik-Orlik et al., 2016; Hidalgo et al., 2020; Luxon, 2011). Also, the frequency of oral mucosal lesions in patients with chronic liver failure was higher compared with the control group (Zahed et al., 2020). However, neither liver cirrhosis nor immunosuppression in liver transplanted patients was identified as risk factor for implant survival (Gu & Yu, 2011; Paredes et al., 2017; Schimmel et al., 2018; Wychowanski et al., 2020), even though liver disease is a risk factor for periodontal disease (Chen et al., 2020) and tooth loss (Yoon et al., 2016). Based on these data, it might be assumed that early peri-implant bone formation is not necessarily impaired in liver cirrhotic patients with their higher risk for osteoporotic fractures and periodontitis. Also, the BDL rat model shows no consistent changes in bone turnover markers (Doustimotlagh et al., 2017, 2018; Veidal et al., 2010) and the impact of BDL on the bone structural parameters is moderate to low (Doustimotlagh et al., 2017; Moradi et al., 2019; Xu et al., 2020).

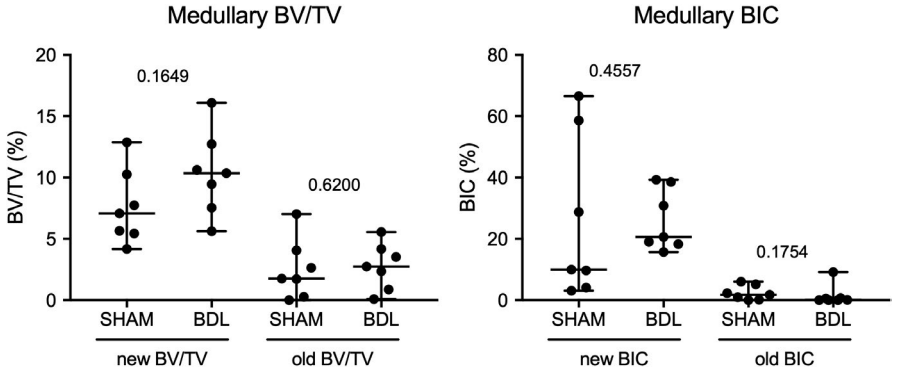

FIGURE 5 Histomorphometric analysis of the implants after healing—the medullary bone. Cirrhosis was induced by bile duct ligation in Wistar rats (BDL) while manipulation but not ligation and dissection were considered SHAM surgery. Four weeks later, implants were inserted in the tibia, and following another four weeks of peri-implant bone formation, histomorphometric analysis was performed. This figure shows results for the medullary region reaching 1 mm into the bone marrow compartment. New and old bone were distinguished based on staining intensity, and "bone volume per tissue volume" (BV/TV) within the region of 200 μm immediately adjacent to the implant surface calculated. "Bone-to-implant contact" (BIC) is a measure for the implant surface covered with bone. Statistical analysis comparing the SHAM and the BDL group was performed using Mann–Whitney U test and the p-valued indicated

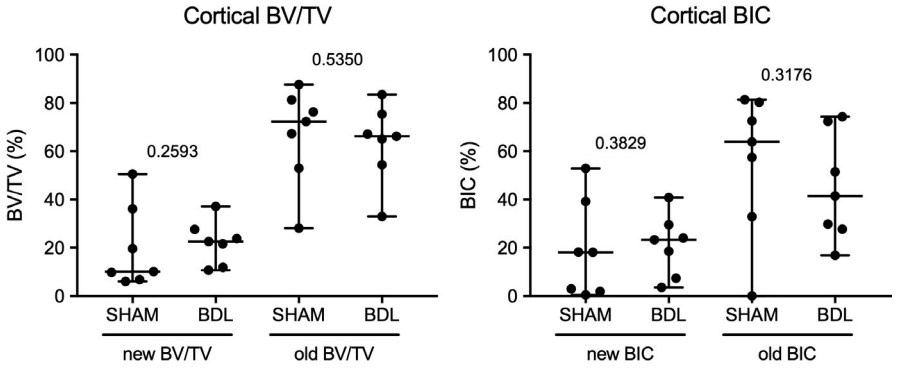

FIGURE 6 Histomorphometric analysis of the implants after healing—the cortical bone. Four weeks after BDL and SHAM surgeries, implants were inserted in the tibia and after another four weeks histomorphometric analysis performed. "Bone volume per tissue volume" (BV/TV) within the region of 200 μm immediately adjacent to the implant surface and "bone-to-implant contact" (BIC) were determined. Statistical analysis comparing the SHAM and the BDL group was performed using Mann–Whitney U test and the p-value indicated

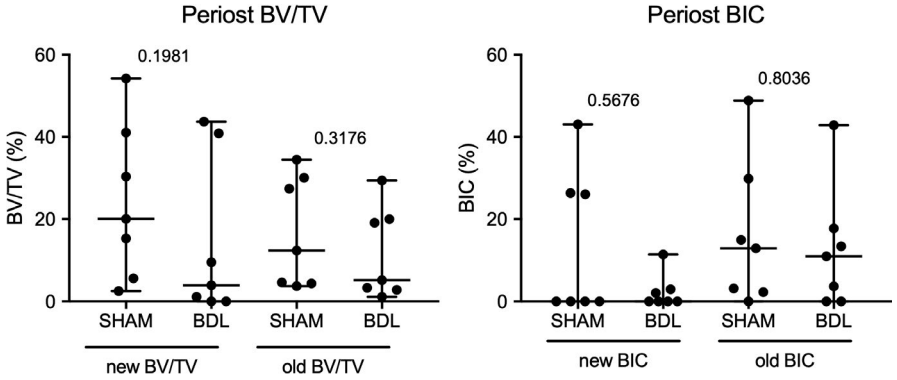

FIGURE 7 Histomorphometric analysis of the implants after healing—the periosteal bone. Four weeks after BDL and SHAM surgeries and another four weeks of peri-implant bone formation, histomorphometric analysis was performed. "Bone volume per tissue volume" (BV/TV) within the region of 200 μm immediately adjacent to the implant surface and "bone-to-implant contact" (BIC) were determined. Statistical analysis comparing the SHAM and the BDL group was performed using Mann–Whitney U test and the *p*-value indicated

Surprisingly, the implication of liver cirrhosis on aspects of bone regeneration, with osseointegration of dental implants being one indication, has not yet been studied.

We show here the histologic and histomorphometric data of peri-implant bone formation in BDL rats. In agreement with previous studies based on a rat tibia implantation model, we observed

peri-implant bone formation of titanium screws in the cortical bone. In support of this claim, the medullary bone formation resembles one of previous studies; for example, BV/TV was around 20% (Kuchler et al., 2013), only slightly higher than the 10% in the present study. The cortical bone formation was approximately 90% in previous studies (Kuchler et al., 2011, 2013), now also reaching 90% when combining new and old bone. Under these conditions, BDL had not caused a significant and relevant change of the standard parameters of peri-implant bone formation—the BV/TV and BIC. Somehow unexpected was the observation that the BDL group even showed a trend toward a higher BV/TV in the medullary compartment than the SHAM group. Taken together, if we relate our findings to those of others, it is obvious that the early stages of peri-implant bone formation are not considerably affected by liver cirrhosis induced by BDL.

The clinical relevance of the data leaves room for speculation. We have to state the four-week BDL causes the cardinal symptoms of cirrhosis including the formation of ascites accumulate liquid in the abdominal cavity, but not necessarily represents the long-term effects that cirrhosis might have on bone healing, a complex process that requires angiogenesis to deliver bone-forming osteoblasts (Sivaraj & Adams, 2016). Even though BDL rats have impaired angiogenesis (Faramarzi et al., 2009), this may not have led to impaired peri-implant bone formation in small defects. However, clinical implant dentistry involves the filling of extraction sockets upon immediate implant placement (Groenendijk et al., 2017) and the possible need for bone augmentation procedures (Thoma et al., 2019). Our findings should not be extrapolated toward large defects. Moreover, the four-week peri-implant bone formation period is considered early as the remodeling in rodents has been started but not reached a steady level; therefore, a possible negative balance on bone remodeling that weakens peri-implant bone formation is not denoted by our model.

Considering that this is a pioneer study linking cirrhosis and peri-implant bone formation, numerous limitations have to be raised. First, the tibia model only moderately represents the situation of the jaw with its unique immunologic situation and the lack of functional loading of implants. Second, our study is a pilot as we have only selected one observation period based on previous studies with PTH (Kuchler et al., 2011; Mair et al., 2009), colitis (Kuchler et al., 2013), and vitamin D deficiency (Dvorak et al., 2012). Future studies should consider the long-term effects of liver cirrhosis on osseointegration. Third, the implants used were titanium screws with a turned surface and it is a rougher surface that might better reflect the clinical scenario. Forth, the impact of ursodeoxycholic acid being one of the first-line therapeutic medications used in the treatment of cholestatic liver disease and taurocholic acid, a conjugation of cholic acid with taurine, both with shown anti-inflammatory properties (Talebian et al., 2020; Talebian et al., 2020) on bone regeneration remains to be determined. Finally, it would be interesting to understand how the deregulation of insulin-like growth factor-1 in BDL rats affects peri-implant bone in the long-term setting (Tarcin et al., 2008).

The present study should be a motivation for additional preclinical and clinical researches to learn more about liver cirrhosis being a possible risk factor in implant dentistry. In conclusion, the presented study shows that cirrhosis induction by BDL has no significant impact on the early stages of peri-implant bone formation in the cortical and medullary compartments in a rat tibia implantation model.

ACKNOWLEDGEMENTS

We thank Toni Dobsak for providing the illustrations, Patrick Heimel for his advice concerning the histomorphometric evaluation, and Nasrin Rahimi for the assistance during BDL surgeries.

AUTHOR CONTRIBUTION

R.T. contributed to conception, design, data acquisition, surgical procedures, interpretation of data, drafted manuscript. C.K. contributed to data acquisition. B.S. contributed to methodology. U.K. contributed to protocol design, surgical procedures. A.R.D. established the preclinical model. R.G. contributed to conception, design, acquisition, analysis, and interpretation of data, drafted manuscript. All authors have critically revised manuscript, and gave final approval.

ORCID

Reza Talebian https://orcid.org/0000-0002-6774-0607
Carina Kampleitner https://orcid.org/0000-0003-3072-5072
Benedikt Sagl https://orcid.org/0000-0002-6739-4222
Ulrike Kuchler https://orcid.org/0000-0001-9744-9856
Reinhard Gruber https://orcid.org/0000-0001-5400-9009

REFERENCES

Algazo, M. A., Amiri-Ghashlaghi, S., Delfan, B., Hassanzadeh, G., Sabbagh-Ziarani, F., Jazaeri, F., & Dehpour, A. R. (2015). Cirrhosis-induced morphological changes in the retina: Possible role of endogenous opioid. *International Journal of Ophthalmology*, *8*(4), 681–684. https://doi.org/10.3980/j.issn.2222-3959.2015.04.07

Chen, Y., Yang, Y. C., Zhu, B. L., Wu, C. C., Lin, R. F., & Zhang, X. (2020). Association between periodontal disease, tooth loss and liver diseases risk. *Journal of Clinical Periodontology*, https://doi.org/10.1111/jcpe.13341

Derakhshanian, H., Ghadbeigi, S., Rezaian, M., Bahremand, A., Javanbakht, M. H., Golpaie, A., Hosseinzadeh, P., Tajik, N., & Dehpour, A. R. (2013). Quercetin improves bone strength in experimental biliary cirrhosis. *Hepatology Research*, *43*(4), 394–400. https://doi.org/10.1111/j.1872-034X.2012.01075.x

Doustimotlagh, A. H., Dehpour, A. R., Etemad-Moghadam, S., Alaeddini, M., Kheirandish, Y., & Golestani, A. (2017). Nitrergic and opioidergic systems affect radiographic density and histomorphometric indices in bile-duct-ligated cirrhotic rats. *Histology and Histopathology*, *32*(7), 743–749. https://doi.org/10.14670/HH-11-836

Doustimotlagh, A. H., Dehpour, A. R., Etemad-Moghadam, S., Alaeddini, M., Ostadhadi, S., & Golestani, A. (2018). A study on OPG/RANK/RANKL axis in osteoporotic bile duct-ligated rats and the involvement of nitrergic and opioidergic systems. *Research in Pharmaceutical Sciences*, *13*(3), 239–249. https://doi.org/10.4103/1735-5362.228954

Dvorak, G., Fugl, A., Watzek, G., Tangl, S., Pokorny, P., & Gruber, R. (2012). Impact of dietary vitamin D on osseointegration in the

ovariectomized rat. *Clinical Oral Implants Research*, *23*(11), 1308–1313. https://doi.org/10.1111/j.1600-0501.2011.02346.x

Faramarzi, N., Abbasi, A., Tavangar, S. M., Mazouchi, M., & Dehpour, A. R. (2009). Opioid receptor antagonist promotes angiogenesis in bile duct ligated rats. *Journal of Gastroenterology and Hepatology*, *24*(7), 1226–1229. https://doi.org/10.1111/j.1440-1746.2009.05794.x

Ghiassy, B., Rahimi, N., Javadi-Paydar, M., Gharedaghi, M. H., Norouzi-Javidan, A., & Dehpour, A. R. (2017). Nitric oxide mediates effects of acute, not chronic, naltrexone on LPS-induced hepatic encephalopathy in cirrhotic rats. *Canadian Journal of Physiology and Pharmacology*, *95*(1), 16–22. https://doi.org/10.1139/cjpp-2016-0188

Gorustovich, A., Angeles Esposito, M., Guglielmotti, M. B., & Juan Giglio, M. (2003). Periimplant bone healing under experimental hepatic osteodystrophy induced by a choline-deficient diet: A histomorphometric study in rats. *Clinical Implant Dentistry and Related Research*, *5*(2), 124–129. https://doi.org/10.1111/j.1708-8208.2003.tb00193.x

Groenendijk, E., Staas, T. A., Graauwmans, F. E. J., Bronkhorst, E., Verhamme, L., Maal, T., & Meijer, G. J. (2017). Immediate implant placement: The fate of the buccal crest. A retrospective cone beam computed tomography study. *International Journal of Oral and Maxillofacial Surgery*, *46*(12), 1600–1606. https://doi.org/10.1016/j.ijom.2017.06.026

Gu, L., & Yu, Y. C. (2011). Clinical outcome of dental implants placed in liver transplant recipients after 3 years: A case series. *Transplantation Proceedings*, *43*(7), 2678–2682. https://doi.org/10.1016/j.transproceed.2011.06.037

Handzlik-Orlik, G., Holecki, M., Wilczynski, K., & Dulawa, J. (2016). Osteoporosis in liver disease: Pathogenesis and management. *Therapeutic Advances in Endocrinology and Metabolism*, *7*(3), 128–135. https://doi.org/10.1177/2042018816641351

Hidalgo, D. F., Boonpheng, B., Sikandar, S., Nasr, L., & Hidalgo, J. (2020). Chronic liver disease and the risk of osteoporotic fractures: A meta-analysis. *Cureus*, *12*(9), e10483. https://doi.org/10.7759/cureus.10483

Hosseini-Chegeni, A., Jazaeri, F., Yousefi-Ahmadipour, A., Heidari, M., Abdollahie, A., & Dehpour, A. R. (2019). Thalidomide attenuates the hyporesponsiveness of isolated atria to chronotropic stimulation in BDL rats: The involvement of TNF-alpha, IL-6 inhibition, and SOCS1 activation. *Iranian Journal of Basic Medical Science*, *22*(11), 1259–1266. https://doi.org/10.22038/ijbms.2019.32256.7742

Kountouras, J., Billing, B. H., & Scheuer, P. J. (1984). Prolonged bile duct obstruction: A new experimental model for cirrhosis in the rat. *British Journal of Experimental Pathology*, *65*(3), 305–311.

Kuchler, U., Luvizuto, E. R., Munoz, F., Hofbauer, J., Watzek, G., & Gruber, R. (2013). Bone healing around titanium implants in two rat colitis models. *Clinical Oral Implants Research*, *24*(2), 224–229. https://doi.org/10.1111/j.1600-0501.2012.02454.x

Kuchler, U., Spilka, T., Baron, K., Tangl, S., Watzek, G., & Gruber, R. (2011). Intermittent parathyroid hormone fails to stimulate osseointegration in diabetic rats. *Clinical Oral Implants Research*, *22*(5), 518–523. https://doi.org/10.1111/j.1600-0501.2010.02047.x

Luxon, B. A. (2011). Bone disorders in chronic liver diseases. *Current Gastroenterology Reports*, *13*(1), 40–48. https://doi.org/10.1007/s11894-010-0166-4

Mair, B., Tangl, S., Feierfeil, J., Skiba, D., Watzek, G., & Gruber, R. (2009). Age-related efficacy of parathyroid hormone on osseointegration in the rat. *Clinical Oral Implants Research*, *20*(4), 400–405. https://doi.org/10.1111/j.1600-0501.2008.01658.x

Mavilia, M. G., Bhardwaj, R., Wakefield, D., & Karagozian, R. (2019). Chronic liver disease patients have worse outcomes and increased postoperative complications after orthopedic fractures. *Journal of Clinical Gastroenterology*, *53*(9), e371–e375. https://doi.org/10.1097/MCG.0000000000001166

Moradi, M., Doustimotlagh, A. H., Dehpour, A. R., Rahimi, N., & Golestani, A. (2019). The influence of TRAIL, adiponectin and sclerostin alterations on bone loss in BDL-induced cirrhotic rats and the effect of opioid system blockade. *Life Sciences*, *233*, 116706. https://doi.org/10.1016/j.lfs.2019.116706

Paredes, V., Lopez-Pintor, R. M., Torres, J., de Vicente, J. C., Sanz, M., & Hernandez, G. (2017). Implant treatment in pharmacologically immunosuppressed liver transplant patients: A prospective-controlled study. *Clinical Oral Implants Research*, https://doi.org/10.1111/clr.13035

Rahimi, N., Hassanipour, M., Allahabadi, N. S., Sabbaghziarani, F., Yazdanparast, M., & Dehpour, A. (2018). Cirrhosis induced by bile duct ligation alleviates acetic acid intestinal damages in rats: Involvements of nitrergic and opioidergic systems. *Pharmacological Reports*, *70*(3), 426–433. https://doi.org/10.1016/j.pharep.2017.11.010

Rybaczek, T., Tangl, S., Dobsak, T., Gruber, R., & Kuchler, U. (2015). The effect of parathyroid hormone on osseointegration in insulin-treated diabetic rats. *Implant Dentistry*, *24*(4), 392–396. https://doi.org/10.1097/ID.0000000000000288

Scaglione, S., Kliethermes, S., Cao, G., Shoham, D., Durazo, R., Luke, A., & Volk, M. L. (2015). The epidemiology of cirrhosis in the United States: A population-based study. *Journal of Clinical Gastroenterology*, *49*(8), 690–696. https://doi.org/10.1097/MCG.0000000000000208

Schimmel, M., Srinivasan, M., McKenna, G., & Muller, F. (2018). Effect of advanced age and/or systemic medical conditions on dental implant survival: A systematic review and meta-analysis. *Clinical Oral Implants Research*, *29*(Suppl 16), 311–330. https://doi.org/10.1111/clr.13288

Schuppan, D., & Afdhal, N. H. (2008). Liver cirrhosis. *The Lancet*, *371*(9615), 838–851. https://doi.org/10.1016/S0140-6736(08)60383-9

Shirazi, M., Ameri, A., Shafaroodi, H., Motahhary, P., Saleh, T., Ghasemi, M., & Dehpour, A. R. (2008). Orthodontic tooth movement in cholestatic and cirrhotic rats. *Journal of Orthodontics*, *35*(2), 119–125, discussion 110–111. https://doi.org/10.1179/146531207225022536

Sivaraj, K. K., & Adams, R. H. (2016). Blood vessel formation and function in bone. *Development*, *143*(15), 2706–2715. https://doi.org/10.1242/dev.136861

Talebian, R., Hashem, O., & Gruber, R. (2020). Taurocholic acid lowers the inflammatory response of gingival fibroblasts, epithelial cells, and macrophages. *Journal of Oral Science*, *62*(3), 335–339. https://doi.org/10.2334/josnusd.19-0342

Talebian, R., Panahipour, L., & Gruber, R. (2020). Ursodeoxycholic acid attenuates the expression of proinflammatory cytokines in periodontal cells. *Journal of Periodontology*, https://doi.org/10.1002/JPER.19-0013

Tarcin, O., Gedik, N., Karakoyun, B., Tahan, V., Sood, G., Celikel, C., & Tozun, N. (2008). Serum prolidase and IGF-1 as non-invasive markers of hepatic fibrosis during four different periods after bile-duct ligation in rats. *Digestive Diseases and Sciences*, *53*(7), 1938–1945. https://doi.org/10.1007/s10620-007-0073-1

Thoma, D. S., Bienz, S. P., Figuero, E., Jung, R. E., & Sanz-Martin, I. (2019). Efficacy of lateral bone augmentation performed simultaneously with dental implant placement: A systematic review and meta-analysis. *Journal of Clinical Periodontology*, *46*(Suppl 21), 257–276. https://doi.org/10.1111/jcpe.13050

Vasak, C., Busenlechner, D., Schwarze, U. Y., Leitner, H. F., Munoz Guzon, F., Hefti, T., Schlottig, F., & Gruber, R. (2014). Early bone apposition to hydrophilic and hydrophobic titanium implant surfaces: A histologic and histomorphometric study in minipigs. *Clinical Oral Implants Research*, *25*(12), 1378–1385. https://doi.org/10.1111/clr.12277

Veidal, S. S., Vassiliadis, E., Bay-Jensen, A. C., Tougas, G., Vainer, B., & Karsdal, M. A. (2010). Procollagen type I N-terminal propeptide (PINP) is a marker for fibrogenesis in bile duct ligation-induced fibrosis in rats. *Fibrogenesis & Tissue Repair*, *3*(1), 5. https://doi.org/10.1186/1755-1536-3-5

Wychowanski, P., Szubinska-Lelonkiewicz, D., Osiak, M., Nowak, M., Kosieradzki, M., & Fiedor, P. (2020). New approach to treatment of

high-risk allograft recipients under chronic immunosuppression with tooth loss. evaluation of safety and longevity of dental implants: A case report. *Transplantation Proceedings*, *52*(8), 2558–2562. https://doi.org/10.1016/j.transproceed.2020.02.103

Xu, X., Wang, R., Wu, R., Yan, W., Shi, T., Jiang, Q., & Shi, D. (2020). Trehalose reduces bone loss in experimental biliary cirrhosis rats via ERK phosphorylation regulation by enhancing autophagosome formation. *The FASEB Journal*, *34*(6), 8402–8415. https://doi.org/10.1096/fj.201902528RRR

Yoon, D. L., Kim, Y. G., Cho, J. H., Lee, S. K., & Lee, J. M. (2016). Long-term evaluation of teeth and implants during the periodic maintenance in patients with viral liver disease. *The Journal of Advanced Prosthodontics*, *8*(4), 321–328. https://doi.org/10.4047/jap.2016.8.4.321

Zahed, M., Bahador, M., Hosseini Asl, M. K., Lavaee, F., Azad, A., & Bahador, A. (2020). Oro-dental health of patients with chronic hepatic failure. *International Journal of Organ Transplantation Medicine*, *11*(3), 115–121.

How to cite this article: Talebian, R., Kampleitner, C., Sagl, B., Kuchler, U., Dehpour, A. R., & Gruber, R. (2021). Bone healing around titanium implants in a preclinical model of bile duct ligation-induced liver injury. *Clinical Oral Implants Research*, 32, 980–988. https://doi.org/10.1111/clr.13792